Origin of ultradian pulsatility in the hypothalamic-pituitary-adrenal axis

Electronic supplementary material (ESM)

Jamie J. Walker[1,*], John R. Terry[1] and Stafford L. Lightman[2]

[1] *Bristol Centre for Applied Nonlinear Mathematics, Department of Engineering Mathematics, University of Bristol, Bristol, United Kingdom*

[2] *Henry Wellcome Laboratories for Integrative Neuroscience and Endocrinology, University of Bristol, Bristol, United Kingdom*

[*] *E-mail: Jamie.Walker@bristol.ac.uk*

Contents

1 Experimental procedures **2**

2 Theoretical methods **2**

2.1 Structure of the theoretical model 2

2.2 Determination of model parameters 5

2.3 Modelling the effects of a GR antagonist 7

2.4 Numerical methods 8

3 Supplementary tables **13**

4 Supplementary figures **14**

1 Experimental procedures

Determination of ultradian rhythmicity in freely moving conscious rats was performed as described in Windle et al. (1998) and Spiga et al. (2007). Essentially the right jugular vein was cannulated and the cannula inserted until it lay close to the entrance of the right atrium. The cannula was then connected to an automated sampling system and 10 - 100 μl blood samples were collected every 10 minutes for 24 hours. Total plasma corticosterone concentrations were measured directly by radioimmunoassay.

2 Theoretical methods

2.1 Structure of the theoretical model

The model takes into account the three major components of the HPA axis and assumes linear mass action kinetics to describe the production and degradation of the primary hormones: corticotrophin releasing hormone (CRH), corticotrophin (ACTH), and CORTicosterone/CORTisol, which are produced by the hypothalamus, anterior pituitary, and adrenal cortex respectively (see Figure 1 of the main text). There is a negative feedback mechanism in the HPA axis whereby CORT, mediated by the glucocorticoid receptor (GR) (Drouin et al. 1992), acts to inhibit further release of ACTH from the anterior pituitary (Jones et al. 1977; Dallman et al. 1987). The nonlinearity introduced by this GR-CORT interaction, as well as incorporation of a delay to account for slow processes involved in ACTH-induced CORT release in the adrenal cortex, turns out to be critical for the generation of ultradian pulsatility in the system.

The equations for the dynamic system were set up as follows. The starting point is the

equations proposed by Gupta et al. (2007):

$$\begin{aligned}
\frac{dC}{dT} &= \frac{K_c + F}{1 + O/k_{i1}} - K_{cd}C, \\
\frac{dA}{dT} &= \frac{K_a C}{1 + OR/k_{i2}} - K_{ad}A, \\
\frac{dR}{dT} &= \frac{K_r (OR)^2}{K + (OR)^2} + K_{cr} - K_{rd}R, \\
\frac{dO}{dT} &= K_o A - K_{od}O,
\end{aligned} \tag{1}$$

where C, A and O represent the concentration levels of CRH (hypothalamus), ACTH (anterior pituitary) and CORT (adrenal cortex) respectively. R represents the availability of GR in the anterior pituitary. The form of these equations was chosen to ensure that all concentrations take positive values. A detailed account of the derivation and justification of system (1) can be found in Gupta et al. (2007).

At this point we made our first simplifying assumption, which was that the rapid inhibition of hypothalamic CRH by CORT is not an important factor. This relates back to the fact that the anterior pituitary is the major site for glucocorticoid feedback (Keller-Wood and Dallman 1984) and the relatively slow effect of glucocorticoids on CRH gene transcription (Ma et al. 1997). This assumption results in a system that is essentially an excitatory-inhibitory loop consisting of the pituitary and adrenal components, which undergoes external forcing due to the action of CRH (see supplementary Figure 7):

$$\begin{aligned}
\frac{dA}{dT} &= \frac{K_a C}{1 + OR/k_{i2}} - K_{ad}A, \\
\frac{dR}{dT} &= \frac{K_r (OR)^2}{K + (OR)^2} + K_{cr} - K_{rd}R, \\
\frac{dO}{dT} &= K_o A - K_{od}O.
\end{aligned} \tag{2}$$

Here C is no longer a variable, but is now a system parameter (with units concentration),

which represents an effective CRH drive on the anterior pituitary. From here, the next step is to nondimensionalize the system, so as to enable a more efficient exploration of model behaviour. We first introduce the dimensionless variables

$$\begin{aligned} t &= K_{od}T, \\ a &= K_{od}^2 K_r^{-1} K_a^{-1} A, \\ r &= K_{od} K_r^{-1} R, \\ o &= K_{od}^3 K_r^{-1} K_a^{-1} K_o^{-1} O, \end{aligned} \tag{3}$$

that upon substitution into (2) lead to the dimensionless system

$$\begin{aligned} \frac{da}{dt} &= \frac{p_1}{1 + p_2 r o} - p_3 a, \\ \frac{dr}{dt} &= \frac{(or)^2}{p_4 + (or)^2} + p_5 - p_6 r, \\ \frac{do}{dt} &= a - o, \end{aligned} \tag{4}$$

where a, r and o are dimensionless representations of the original concentrations A, R and O respectively, and the parameters p_i are dimensionless combinations of the original parameters, defined as follows:

$$\begin{aligned} p_1 &= K_{od} K_r^{-1} C, \\ p_2 &= K_r^2 K_a K_o K_{i2}^{-1} K_{od}^{-4}, \\ p_3 &= K_{ad} K_{od}^{-1}, \\ p_4 &= K K_{od}^8 K_r^{-4} K_a^{-2} K_o^{-2}, \\ p_5 &= K_{cr} K_r^{-1}, \\ p_6 &= K_{rd} K_{od}^{-1}. \end{aligned} \tag{5}$$

Note that an increase/decrease in CRH drive on the anterior pituitary corresponds to increasing/decreasing parameter p_1. Thus in the main text, we refer to parameter p_1 as 'CRH drive'.

Although ACTH and CORT are both synthesized by glandular cells, their mechanisms of release are quite different. In the anterior pituitary following synthesis, ACTH is stored in granules in the readily releasable pool near the cell membrane. Following stimulation by CRH, this pre-synthesized ACTH is rapidly released into the blood. In the adrenal cortex, however, CORT is only synthesized following stimulation by ACTH, after which it is released into the blood. This results in a delay, T_{lag} (units minutes) say, in ACTH induced CORT release from the adrenal cortex (Papaikonomou 1977). From a modelling perspective, to take into account this slow process in the adrenal cortex, we include a delay term in the equation for CORT, which results in the following delay differential equation (DDE)

$$\begin{aligned} \frac{da}{dt} &= \frac{p_1}{1+p_2 ro} - p_3 a, \\ \frac{dr}{dt} &= \frac{(or)^2}{p_4 + (or)^2} + p_5 - p_6 r, \\ \frac{do}{dt} &= a\,(t-\tau) - o. \end{aligned} \tag{6}$$

The third equation of (6) states that the rate of change of CORT (o) depends on the concentration of ACTH (a) at some amount of (dimensionless) time τ earlier.

2.2 Determination of model parameters

The deterministic (i.e. non-stochastic) dynamics of (6) is governed solely by the parameters of the system. Of these, we treat only p_1 as a time-varying parameter as it corresponds to CRH drive on the anterior pituitary. We assume that all other parameters of (6), namely p_2, p_3, p_4, p_5, p_6, and τ, would remain constant (at least over a timescale of days) in any individual rat, although of course some inter-individual variation would certainly occur. Whilst it is not possible to determine all of these fixed model parameters from data, approximations are possible for some. The advantage of this approach is that it reduces

the number of free parameters and thus allows a more systematic analysis of the model's behavior.

In particular, the half lives of ATCH and CORT in the blood have been reported in previous experimental studies. In the rat, Papaikonomou (1977) estimated the half life of ACTH ($ACTH_{1/2}$) to be in the range $0.5-1$ minutes. The form of (2) is such that (in the absence of CRH, CORT and GR) ACTH is assumed to decay exponentially at a rate governed by the parameter K_{ad}, which enables us to determine the decay rate for ACTH as

$$K_{ad} = \frac{\ln(2)}{ACTH_{1/2}}. \tag{7}$$

Similarly, Windle et al. (1998) estimated the half life of CORT in the rat ($CORT_{1/2}$) to be in the range $7.2-10$ minutes. This gives the decay rate of CORT as

$$K_{od} = \frac{\ln(2)}{CORT_{1/2}}. \tag{8}$$

Referring back to the relationship between parameters in dimensional and dimensionless form (5), this enables us to determine

$$p_3 = \frac{K_{ad}}{K_{od}} = \frac{CORT_{1/2}}{ACTH_{1/2}}. \tag{9}$$

Furthermore, it gives us the relationship between timescales (3) as

$$t = K_{od}T = \frac{\ln(2)}{CORT_{1/2}}T. \tag{10}$$

In addition to the half-lives of ACTH and CORT, the delay in ACTH-induced CORT release from the adrenal gland of the rat has also been investigated experimentally (Papaikonomou 1977). From a modelling perspective, we consider the delay in ACTH-induced CORT release within the adrenal cortex of the rat to be in the range $T_{lag} = [0, 20]$ minutes. Using (10), this translates to a range in the dimensionless delay of $\tau = [0, 1.9254]$. Note that

in the main text, we present time in its dimensional form (with units of minutes) but all other variables are presented in their dimensionless form (with arbitrary units).

Our analysis (discussed in detail in the following section) focuses on studying the response of the pituitary-adrenal system to exogenous hypothalamic CRH drive and the effects of the delay on this response. We therefore treat p_1 and τ as free parameters, but choose to fix all others to those values given in Table 1. Whilst this particular choice of fixed parameters leads to ultradian oscillations of similar frequency to those recorded experimentally, it is important to stress that other choices are also capable of giving oscillations at physiological frequencies.

2.3 Modelling the effects of a GR antagonist

We assume binding of the GR antagonist (R_A) to the receptor (R) can be described by the straightforward reaction equation (assuming the dissociation rate is very slow in comparison to the asssociation rate)

$$[R] + [R_A] \xrightarrow{\alpha} [RR_A]. \tag{11}$$

Applying the law of mass action leads to the differential equation

$$[\dot{R}] = -\alpha[R][R_A] \tag{12}$$

$$\Rightarrow [\dot{R}] = -\gamma[R] \quad \text{where} \quad \gamma = \alpha[R_A] = constant, \tag{13}$$

since the GR antagonist is infused at constant high levels. The result of this is that the second equation of (2), describing the dynamics of GR, becomes

$$\frac{dR}{dT} = \frac{K_r\,(OR)^2}{K + (OR)^2} + K_{cr} - (K_{rd} + \gamma)\,R. \tag{14}$$

Thus, from a modelling perspective, infusing a GR antagonist is equivalent to increasing the dimensionless parameter $p_6 = K_{rd}K_{od}^{-1}$. In Figure 6*b* of the main text we used $p_6 = 2.8$ (VEH) and $p_6 = 3.3$ (GR antagonist Org 34850).

2.4 Numerical methods

In order to enable swift reproduction of our results, in this section we summarize the numerical methods used in the analysis of the DDE (6). In addition, all code is available on request. For a more detailed discussion on numerical analysis of DDEs we recommend Chapter 5 of the book by Kane and Shore (2005); we now provide a brief summary of the relevant sections.

System (6) is a delay differential equation (DDE) with a single fixed delay $\tau > 0$, and takes the more general form

$$\dot{\mathbf{x}} = f\left(\mathbf{x}\left(t\right), \mathbf{x}\left(t-\tau\right), P\right) \equiv f\left(u, v, P\right), \tag{15}$$

where $\mathbf{x} = (a, r, o)$, f is a nonlinear function corresponding to the right-hand-side of (6) and P is the set of parameters $p_1, p_2, \ldots, p_6$. A steady state solution $\mathbf{x}_0$ of (15) is found by setting the right-hand side of (15) to zero, which in terms of (6) is equivalent to a constant equilibrium in levels of a, r and o. The stability of a steady state is then determined by the eigenvalues of the characteristic equation

$$\det\left(\lambda I - A_1 - A_2 e^{-\lambda\tau}\right) = 0 \tag{16}$$

where

$$A_1 = \frac{\partial f\left(\mathbf{x}_0\right)}{\partial u} \quad , \quad A_2 = \frac{\partial f\left(\mathbf{x}_0\right)}{\partial v} \tag{17}$$

and I is the identity matrix. The delay leads to a transcendental characteristic equation with infinitely many solutions (eigenvalues), which exist either as single real numbers or as

complex congugate pairs. A steady state is stable if all its eigenvalues have negative real part, and unstable if any eigenvalues have positive real part. As parameters of the system vary, the eigenvalues move through the complex plane. Regarding this study, if on varying a parameter a conjugate pair of complex eigenvalues cross the imaginary axis, a transition from a constant response to a pulsatile response (termed a Hopf bifurcation) occurs (Kuznetsov 1995). The Hopf bifurcation is called supercritical if the resulting pulsatile solution is stable.

The transcendental nature of the characteristic equation for a DDE with a fixed delay does not lend itself well to analytical study. Recently, numerical methods have become the method of choice for studying systems with delay, and the two key approaches are outlined below.

Numerical simulation

Time series of (6) are obtained by numerical simulation, which allows us to gain some intuition about a system. The task of numerically simulating a DDE is fairly simple. For a DDE with a fixed delay τ it is best to use a fixed time step, h say. We firstly discretise the history interval $[-\tau, 0]$ into N equidistant intervals such that $h = \tau/N$. In performing a computation we must firstly initialise and then continue to store all $N + 1$ computed points in the interval $[-\tau, 0]$. In the study of (6) we used an Adams-Bashforth fourth-order multistep integrator (Press et al. 2007), where the next point in time x_n is calulated using the previous four points:

$$x_n = x_{n-1} + \frac{h}{24}\left(55x'_{n-1} - 59x'_{n-2} + 37x'_{n-3} - 9x'_{n-4}\right)$$

The prime means take the derivative with respect time. In order to implement this routine for a DDE, we had to increase the history interval by three extra elements to $[-\tau - 3\tau/N, 0]$. This integrating routine was used to produce all time series in the main text; namely Figure 3*b,c,d*, Figure 5*c,d,e,f*, and Figure 6*b*.

For those time series where a circadian or ultradian CRH drive was considered, the CRH profile took the following form (note dimensionless time):

$$p_1 = B + A\sin(\omega t) + \text{noise}$$

In Figure 5*c* of the main text and supplementary Figure 8 we used $B = 16$, $A = 1$ and $\omega = 2\pi/138.6294$; and in Figures 5*d* and 6*b* of the main text we used $B = 26$, $A = 10$ and $\omega = 2\pi/138.6294$ with zero noise. In Figure 5*e* of the main text we used $B = 26$, $A = 1$ and $\omega = 2\pi/1.9254$ with zero noise; and in Figure 5*f* of the main text we used $B = 10$, $A = 1$ and $\omega = 2\pi/1.9254$ with zero noise.

Numerical continuation

A more advanced method is that of numerical continuation (Kuznetsov 1995; Krauskopf et al. 2007). The idea is to identify some parameter values where there is a qualitative change in the dynamics (for example a Hopf bifurcation). Using a continuation software package, we can then follow this bifurcation in one or more parameters through parameter space. This results in a curve in parameter space with qualitatively different dynamics on either side. A collection of these curves constitutes a bifurcation diagram. Here we employed a numerical continuation package written for MATLAB (MathWorks) called DDE-BIFTOOL (Engelborghs et al. 2001), designed for bifurcation analysis of DDEs with constant (and state-dependent) delays. DDE-BIFTOOL lets us follow steady states and periodic orbits independent of their stability. It can also follow local codim 1 bifurcations of steady states (for example Hopf bifurcations), but can currently only detect codim 1 bifurcations of periodic orbits. In addition to local bifurcations of steady states, DDE-BIFTOOL can also follow curves of homoclinic and heteroclinic loops, which often play an important role in the overall organisation of bifurcation diagrams. In this work we used DDE-BIFTOOL to compute the Hopf curve (which we term the 'transition curve' in the main text) - dividing (adrenal delay, CRH drive)-parameter space into regions of constant and pulsatile response - in Figures 3*a* and 5*a* of the main text. We also used DDE-BIFTOOL to continue the periodic orbits (and compute their period) in Figure 4 of

the main text.

References

M. F. Dallman, S. F. Akana, C. S. Cascio, D. N. Darlington, L. Jacobson, and N. Levin. Regulation of ACTH secretion: variations on a theme of B. *Recent Prog. Horm. Res.*, 43:113–173, 1987.

J. Drouin, Y. L. Sun, S. Tremblay, P. Lavender, T. J. Schmidt, A. de Léan, and M. Nemer. Homodimer formation is rate-limiting for high affinity DNA binding by glucocorticoid receptor. *Mol. Endocrinol.*, 6(8):1299–1309, 1992.

K. Engelborghs, T. Luzyanina, and G. Samaey. DDE-BIFTOOL v. 2.00: a Matlab package for bifurcation analysis of delay differential equations. Technical report tw-330, Department of Computer Science, K.U. Leuven, Leuven, Belgium, 2001.

S. Gupta, E. Aslakson, B. M. Gurbaxani, and S. D. Vernon. Inclusion of the glucocorticoid receptor in a hypothalamic pituitary adrenal axis model reveals bistability. *Theor. Biol. Med. Model.*, 4(8), 2007.

M. T. Jones, E. W. Hillhouse, and J. L. Burden. Dynamics and mechanics of corticosteroid feedback at the hypothalamus and anterior pituitary gland. *J. Endocrinol.*, 73(3):405–417, 1977.

D. M. Kane and K. A. Shore. *(Eds.) Unlocking Dynamical Diversity: Optical Feedback Effects on Semiconductor Lasers*. Wiley, 2005.

M. E. Keller-Wood and M. F. Dallman. Corticosteroid inhibition of acth secretion. *Endocr. Rev.*, 5(1):1–24, 1984.

B. Krauskopf, H. M. Osinga, and J. Galán-Vioque. *(Eds.) Numerical Continuation Methods*

for Dynamical Systems: Path following and boundary value problems. Springer-Verlag, 2007.

Y. A. Kuznetsov. *Elements of Applied Bifurcation Theory*. Springer-Verlag, New York, 1995.

X. M. Ma, A. Levy, and S. L. Lightman. Rapid changes of heteronuclear rna for arginine vasopressin but not for corticotropin releasing hormone in response to acute corticosterone administration. *J. Neuroendocrinol.*, 9(10):723–728, 1997.

E. Papaikonomou. Rat adrenocortical dynamics. *J. Physiol.*, 265:119–131, 1977.

W. H. Press, S. A. Teukolsky, W. T. Vetterling, and B. P. Flannery. *Numerical Recipes: The Art of Scientific Computing*. Cambridge University Press, third edition, 2007.

F. Spiga, L. R. Harrison, S. A. Wood, H. C. Atkinson, C. P. MacSweeney, F. Thomson, M. Craighead, M. Grassie, and S. L. Lightman. Effect of the glucocorticoid receptor antagonist org 34850 on basal and stress-induced corticosterone secretion. *J. Neuroendocrinol.*, 19:891–900, 2007.

R. J. Windle, S. A. Wood, N. Shanks, S. L. Lightman, and C. D. Ingram. Ultradian rhythm of basal corticosterone release in the female rat: Dynamic interaction with the response to acute stress. *Endocrinology*, 139(2):443–450, 1998.

3 Supplementary tables

Parameter	Value	Description
p_1	Free parameter	Relates to CRH drive
p_2	15	Relates to inhibition by CORT on release of ACTH
p_3	7.2	Ratio of (dimensional) decay rates between ACTH and CORT
p_4	0.05	Relates to synthesis rate of GR governed by OR
p_5	0.11	Basal production of GR in the anterior pituitary
p_6	2.9	Ratio of (dimensional) decay rates between GR and CORT
τ	Free parameter	Delay in ACTH-induced CORT release

Table 1. Dimensionless parameter values for the model.

4 Supplementary figures

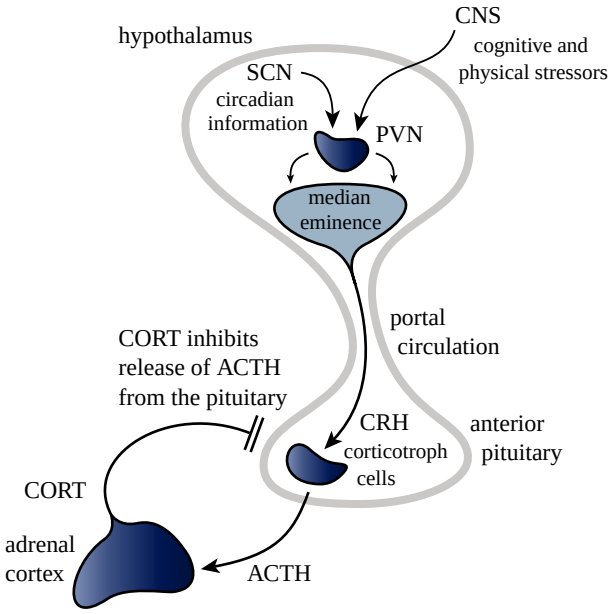

Figure 7. The pituitary-adrenal system. Evidence suggests that the anterior pituitary is the major site for glucocorticoid feedback (Keller-Wood and Dallman 1984). Furthermore, glucocorticoids have a relatively slow effect on CRH gene transcription (Ma et al. 1997). Therefore, we consider the pituitary-adrenal system as an excitatory-inhibitory loop which undergoes external forcing due to the action of CRH.

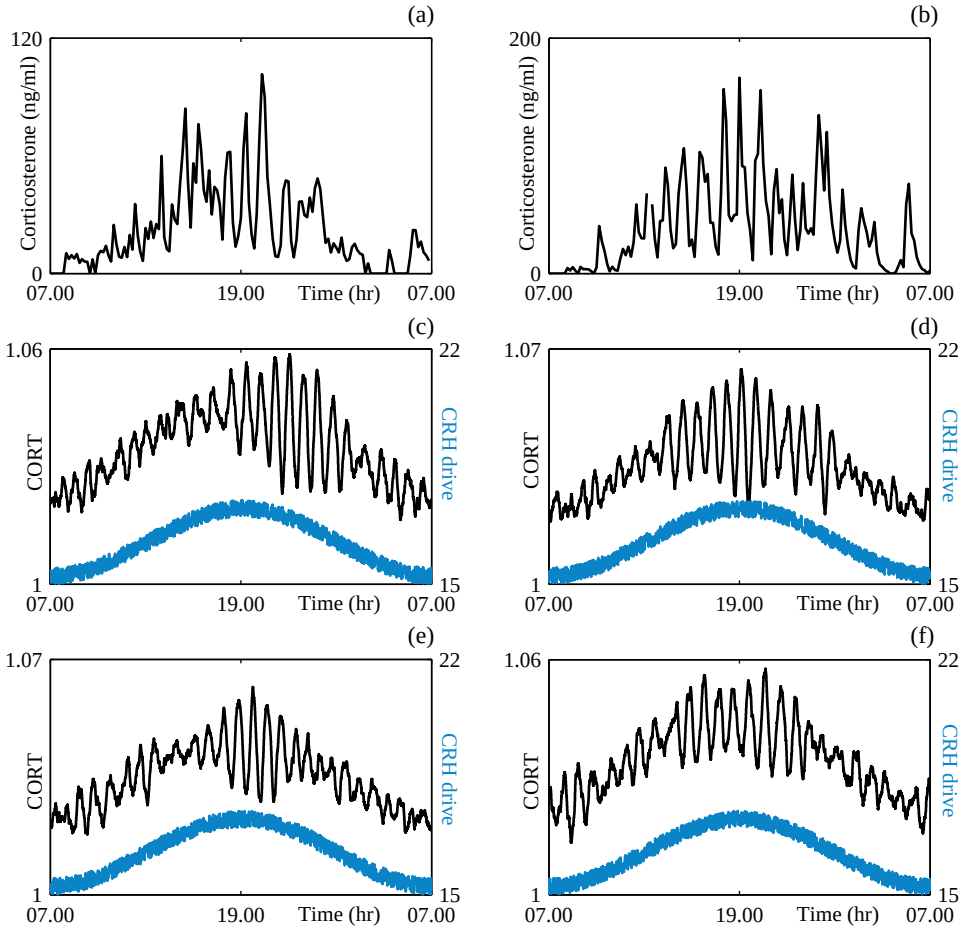

Figure 8. Comparison of experimental data with model predictions. (a,b) Experimental data demonstrating the ultradian glucocorticoid rhythm underlying the classic circadian profile. Levels of blood corticosterone were recorded over a 24hr period in two individual male Sprague-Dawley rats. Blood samples were collected every 10 minutes using an automated blood sampling system. Grey bars indicate the dark phase (19.15 - 05.15 hr). Data from Spiga et al. (2007). (c-f) Model predictions demonstrating noise-induced coherent oscillations (NICO) during the peak of the circadian CRH drive. Computed with a delay of 9.4 min. (Units of all model hormone levels are arbitrary).